Statistics of Solar Cycle–La Niña Connection: Correlation of Two Autocorrelated Time Series

EDDIE HAAM

Department of Applied Mathematics, Harvard University, Cambridge, Massachusetts, and Department of Applied Mathematics, University of Washington, Seattle, Washington

KA-KIT TUNG

Department of Applied Mathematics, University of Washington, Seattle, Washington

(Manuscript received 31 March 2012, in final form 25 May 2012)

ABSTRACT

Both the 11-yr solar cycle and the El Niño–Southern Oscillation (ENSO) phenomena are quasi periodic, with periods of 9–11 and 3–4 yr, respectively. There have been claims that the two are correlated, with the sun at its peak in sunspot number presumably forcing a cold event in the equatorial Pacific. However, both phenomena are also highly autocorrelated. Caution should be exercised when testing for the statistical significance of the correlation of two autocorrelated time series. The solar peak years can coincide with cold ENSO by chance, even if the two time series are independent, and the coincidence then persists for many cycles due to their autocorrelation, before drifting apart. This study demonstrates that this is indeed the case using the Quinn El Niño index (1525–1987), which is a chronicle of observations of El Niño–related events, and the sunspot number (SSN) series going back to 1750. Appropriate statistical tests are suggested that can test for correlation, taking into account autocorrelation applicable to the shorter instrumental records. There is so far no solar peak–La Niña connection found that is statistically significant.

1. Introduction

Since 1979, total solar irradiance (TSI) has been observed by spaceborne satellites to undergo an approximate 11-yr variation of about 0.1% from minimum (''solar min'') to maximum (''solar max'') (Lean et al. 2005). Prior to 1979, various proxies were used to characterize this quasi-periodic variation in solar radiation reaching the Earth. Among them is the sunspot number (SSN). Continuous monthly averages of SSN have been available at the Royal Observatory of Belgium since 1749 (online catalogue of the sunspot index at http://sidc.oma.be/html/sunspot.html). Although TSI and SSN generally follow each other—either can be used to characterize solar max or solar min—there is some difference in detail. While solar max tends to have a broad maximum in TSI, there is a peak in SSN early in the solar max that is not reflected in the radiation change. The physical significance of the SSN peak in terms of radiation reaching Earth is not clear.

Van Loon et al. (2007) and Van Loon and Meehl (2008) found that when the sea surface temperature (SST) in 11 SSN peak years were composited, there appears a surprisingly strong (almost 1 K) La Niña–like cold tongue in the eastern equatorial Pacific, relative to a climatology. The result continued to hold when three more solar cycles were added. This result, if true, could potentially provide, through ENSO and its global influence, the missing mechanism that amplifies the small solar-cycle radiative forcing to produce a large-scale response that can affect global climate and weather. Composites based on TSI in the broad solar max years do not yield the same result, and multiple regression methods based on TSI yield only minor warming (Roy and Haigh 2010; Tung and Zhou 2010) and produce composite mean patterns that are not statistically significant (Zhou and Tung 2010) in the same region. ENSO-like signals (but with various phases) have also been produced in climate models forced with variations in TSI (Meehl et al. 2009; Meehl and Arblaster 2009). A recent modeling result (Misios and Schmidt 2012) found only minor warming, consistent with Tung

Corresponding author address: Eddie Haam, School of Engineering and Applied Sciences, Harvard University, Cambridge, MA 02138.
E-mail: keh@eecs.harvard.edu

DOI: 10.1175/JAS-D-12-0101.1

and Zhou (2010). No modeling result is available with SSN forcing, to the extent that SSN is different from TSI.

Meehl and Arblaster (2009) additionally found that the cold ENSO at SSN peak years is followed 2–3 yr later by a ''lagged warm event.'' This result was recently reexamined by Roy and Haigh (2012). Of the 14 solar cycles in that period, they identified that 9 peak SSN years are associated with a negative ENSO-3.4 index (with cold equatorial SST in the region 5°S–5°N, 120°–170°W). Of the nine solar cycles that are cold at SSN peak, four remain cold for the following 2 yr and five become warm after 1 or 2 yr. So the lagged warm events are not statistically significant. The analysis of White and Liu (2008) of a shorter record happens to have excluded all four cases that remain cold, and they found a cluster of cold-to-warm evolution in the latter half of the twentieth century, as pointed out by Roy and Haigh (2012). We will not be examining this evolution, but we mention it here as an example of the possible clustering effect.

Since ENSO can exist without solar forcing, and (of course) vice versa, the possibility of two time series lining up by accident and then having the correlation persist for many cycles needs to be considered and common Student's *t* tests do not address this case (e.g., Awe 1964). Consider the idealized case of two sine time series, one with an 11-yr period (''solar cycle'') and one with a 3.7-yr period (''ENSO'') (see Fig. 1). If we pick only one year out of each ''solar cycle''—say, at the peak of the sine—and look at whether ''ENSO'' is positive or negative during that year (and not at a particular point in the latter's cycle), then we see that there are long periods when the peak in the ''solar cycle'' is associated with ''cold ENSO.'' In fact, in this example, and with this particular initial condition, this occurs in nine ''solar peak'' years before the correlation switches sign. In a short record comprising 14 ''solar cycles,'' the occurrence of ''cold ENSO,'' 9 out of 14, may seem more significant than the ''random 50–50'' (more on this later). It is common for these accidental correlations that when we look at longer records, they either fall apart or switch to a correlation of the opposite sign (i.e., becoming ''warm ENSO'' at ''solar peak''). Of course, the real ENSO does not have a fixed period and there is some randomness in phase. So, we do not expect consecutive correlations of nine in a row in the real data. Nevertheless, this example demonstrates the property of two autocorrelated time series reverting to the mean of 50–50 when sufficiently long records are examined, despite a much higher probability of getting one sign in a shorter record.

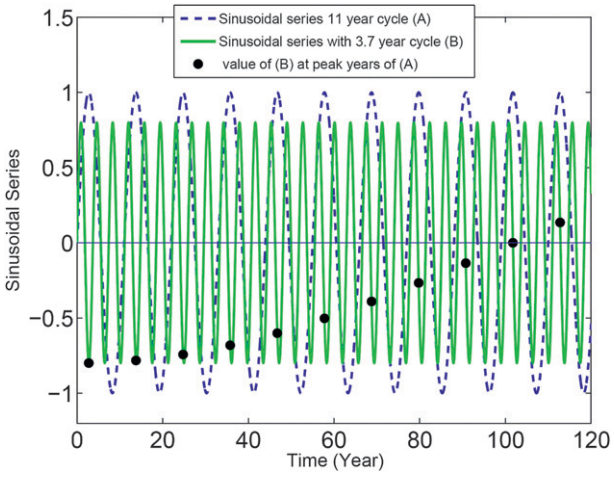

FIG. 1. Two sine waves. The dashed line is a sine wave with a period of 11 yr, and the solid line is a sine wave with a period of 3.7 yr. The solid circles mark the value of the shorter-period sine curve at the time when the longer-period sine reaches its peak.

2. Quinn El Niño

The Quinn index (Quinn 1992; Ortlieb 2000) (1525–1987) is constructed based on a collection of documented incidence of El Niño–related events, such as travel times between ports along the coast of Peru and ship logs noting unusual sea and weather conditions, abnormally high air temperatures in the coastal cities of northern Peru, and significant rises in sea level. It describes annual conditions, but it also notes the change in ENSO categories within a year. None of the mixed categories involves neutral or cold ENSO, since they are not differentiated: The series is categorized from 0 (neutral or cold ENSO) to 6 (strong El Niño). Cold ENSO (La Niña) is not separately characterized.

Figure 2 shows that during the period 1750–1987, when continuous SSN records are available, there are 21 peak SSN years. At 12 of those times, ENSO is a category 0, either neutral or cold. If all category 0 cases of the Quinn index are taken as cold, then the maximum possible number of cold-ENSO cases is 12 at 21 SSN peak years. Under the assumption that there is a 50% chance to be at cold ENSO at each solar peak year, the *p* value of the ratio of 12/21 or higher [e.g., $P(X \geq 12)$] can be shown, using cumulative binomial distribution, as

$$\begin{aligned} P(X \geq 12) &= 1 - P(X \leq 11) \\ &= 1 - \sum_{i=0}^{11} \binom{21}{i} 0.5^i 0.5^{21-i} \\ &= 1 - 0.67 = 0.33. \end{aligned}$$

This value is too high to reject the null hypothesis that there is no solar–La Niña association; we could alternatively say that the null hypothesis can be rejected at only 67% confidence level. In addition, the actual *p*

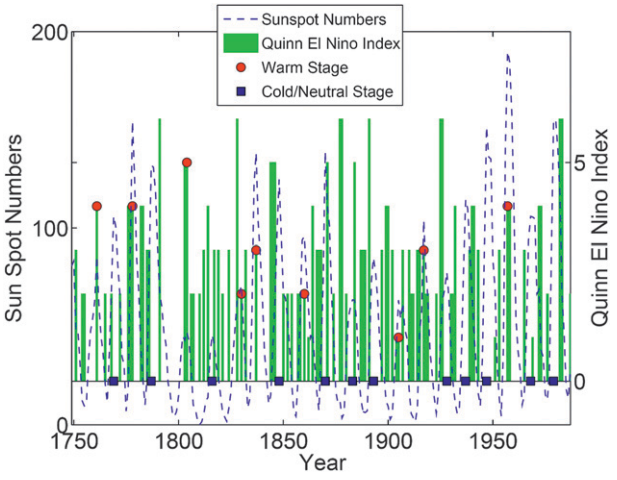

FIG. 2. The Quinn El Niño index (solid bars; right ordinate), used as an El Niño proxy, and the SSNs (dashed curve; left ordinate), for years 1750–1987. The strongest El Niño events are category 6 and the neutral or cold ENSO are category 0. The values of the Quinn index at SSN peak years are marked with solid circles for positive ENSO (El Niño) years and solid squares for either neutral or negative ENSO (La Niña) years.

value is likely to be much larger than 0.33 because of the autocorrelation of ENSO data and the fact that a few of the category 0 of ENSO cases can be considered as neutral instead of cold. In fact, 3 of the 12 category 0 years, the ones that occur in the recent instrumental record, are probably neutral, using the ENSO-3.4 index (see Fig. 4). Although the two indices do not always coincide because of the differences in geographical location (Quinn index to the west of the ENSO-3.4 index), it is nevertheless reasonable to assume that the percentage of neutral cases is the same in the two indices during the modern period. An alternative is to reconstruct the Quinn index by replacing the proxy data with instrumental records during the modern era, with the same result as with the assumption. It is quite likely that over the 21 solar peak years, the warm- and cold-ENSO years are evenly distributed at 9 each.

We should also note this distribution of category 0 cases of the Quinn index: more cold/neutral stages are found at SSN peaks years after 1860 than the years before 1860. This pattern is similar to the clustering of cold-ENSO years shown in Fig. 1, but when longer time periods are considered, the ratio of cold to warm cases approaches 1.

One could argue that the Quinn index may not be accurate enough. Next, we will test the instrumental records, such as the cold tongue index and the ENSO-3.4 index. With these shorter records, we will not be able to see the reversion to the long-term mean, but there are methods that allow one to test for statistical significance while taking into account autocorrelation that could give rise to a high accidental correlation.

3. Statistical tests

One does not always have the luxury of a long enough data record to see if the accidental correlation in shorter records degenerates. Fortunately, there are statistical tests, which are a little more sophisticated than what was used so far, to address this problem. These tests can be applied to limited records. There are two different types of tests. One tests if the amplitude of the cold temperature is different from zero. The other tests if the frequency of occurrence of cold-ENSO events is higher than by random chance. The Student's t test used by Van Loon et al. (2007) and Van Loon and Meehl (2008) is amplitude based. It is sensitive to the climatology used to define the anomaly amplitude. In Van Loon et al. (2007) the climatology was based on only 30 yr (1950–79), while in Van Loon and Meehl (2008) the climatology used was based on 29 yr (1968–96). The anomaly amplitude to be tested was obtained by subtracting this climatology from the average of the temperature in the 11 or 14 solar peak years, and the Student's t test found the signal to be significant at the 95% confidence level. Zhou and Tung (2010) showed that, since the temperature in the chosen periods for defining climatology was warmer than the period of the composite, the anomaly then appeared cold. They further showed that the anomaly did not pass the Student's t test if the climatology was based on the whole period of the data used (1854–2007).

The frequency of the occurrence-based test that we will use is not sensitive to the amplitude of the signal and so the choice of climatology in defining the signal is less important. It, however, is sensitive to the threshold used to define a cold- or warm-ENSO occurrence. We will show by changing the definition of the threshold that our results remain robust.

The null hypothesis of the test is that ENSO is not at the cold stage at SSN peak years. The test statistic is the number of cold winters at SSN peaks. The null distribution is computed by randomizing the ENSO time series. The SSN time series is the same as the observed one. When randomizing the time series, we will account for the autocorrelation structure and frequency content of the ENSO cycles. An observed correlation is statistically significant at the 95% confidence level if the random null distribution achieves such a correlation or higher in only 5% of the test cases (i.e., p value = 0.05).

The Student's t test used by Van Loon et al. (2007) assumes a white-noise distribution for the occurrence of ENSO, with no autocorrelation. Roy and Haigh (2012)

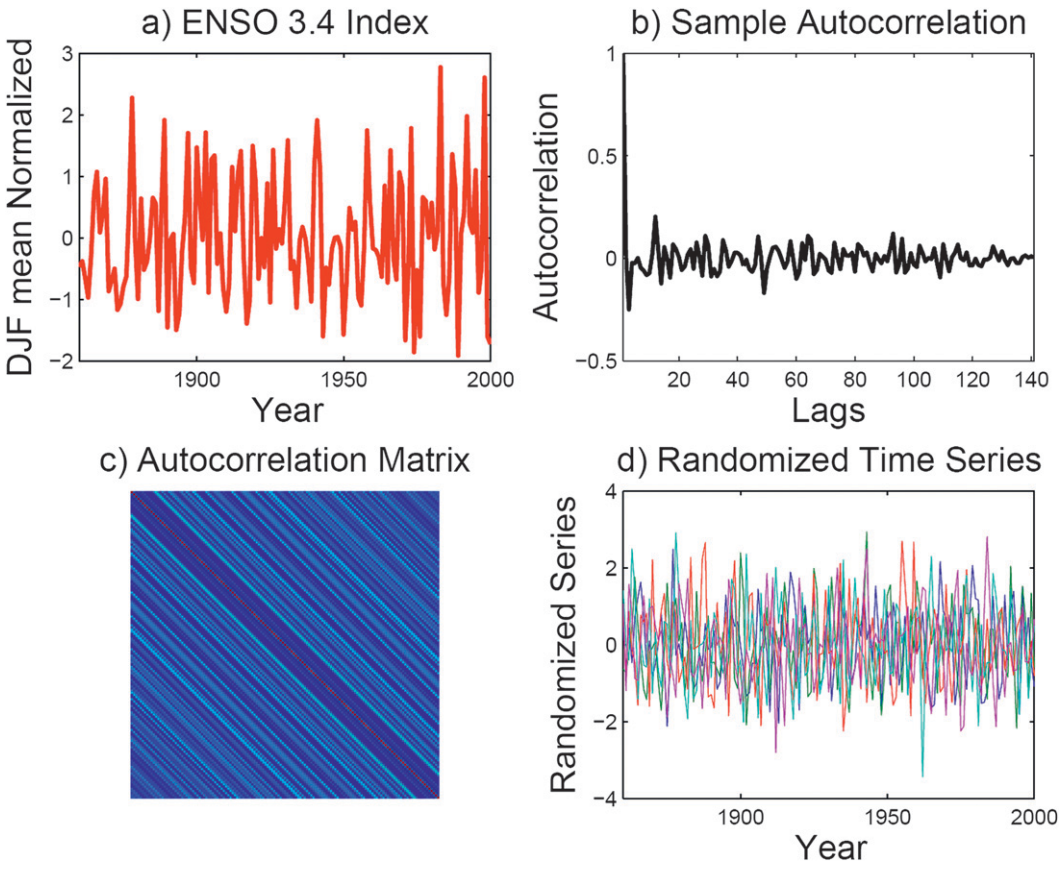

FIG. 3. The steps to generate randomized time series that carry the same distribution and autocorrelation as those of (a) the ENSO-3.4 index. (b) First, the sample autocorrelation is generated. (c) Second, an autocorrelation matrix is created, where the *n*th off-diagonal term is set to the *n*th lag year autocorrelation. (d) Third, the Cholesky decomposition of the matrix in (c) is then multiplied by the univariate random number, which is sampled using inverse transform sampling technique, to produce the randomized series that carry the same distribution and expected autocorrelation as those of the ENSO-3.4 index.

recognizes the autocorrelation of the ENSO time series and attempts to estimate it using an first-order autoregressive [AR(1)] process. Different ways of estimating the AR(1) coefficients could yield different magnitudes for the coefficients. Since we are interested in testing one particular realization of ENSO (the observed one), and not the stochastic system that produced the ENSO, it is more accurate to use the exact sample autocorrelation of ENSO instead of that estimated from an AR(1) process. The randomized ENSO series is generated here using the Cholesky decomposition method (Haam and Huybers 2010), so that the randomized ENSO series carry the same expected autocorrelation [and thus the same expected power spectrum as the ENSO series according to the Wiener–Khinchin theorem (e.g., Percival and Walden 1993; Schreiber and Schmitz 1996; Wunsch 1999)]. We have also considered surrogate series generation by randomizing either phase, amplitude, or both, of the Fourier transformed data (Schreiber and Schmitz 2000; Wunsch 1999). However, depending on the nature of the data, the distribution and the autocorrelation of the surrogates are not always the same as those of the sample series (e.g., Rapp et al. 1994; Theiler et al. 1992; Schreiber and Schmitz 1996). So these latter methods are not used here.

The first step of the Cholesky decomposition method (Haam and Huybers 2010), as shown in Fig. 3, is to calculate the sample autocorrelation (Fig. 3b) of, for example, the ENSO-3.4 index (Fig. 3a) as a function of lag years. Then the autocorrelation matrix is constructed where the *n*th off-diagonals terms are equal to the *n*th autocorrelation function (i.e., autocorrelation with *n*-year lag) with *n* ranging from 0 to $N - 1$, where N is the total number of years in the record (Fig. 3c). The Cholesky decomposition of the autocorrelation matrix is applied and then multiplied by the univariate random numbers, which were sampled using inverse transform sampling (Devroye 1986), in order to generate random time series

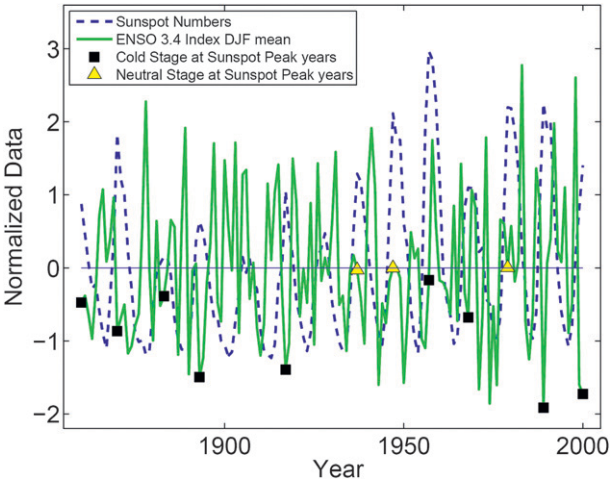

FIG. 4. The ENSO-3.4 index (solid line) and the SSN (dashed line). Cold-ENSO cases at sunspot peak years are marked by squares, while neutral-ENSO cases (defined as within ±0.02 units of the mean index) at sunspot peak years are marked with triangles.

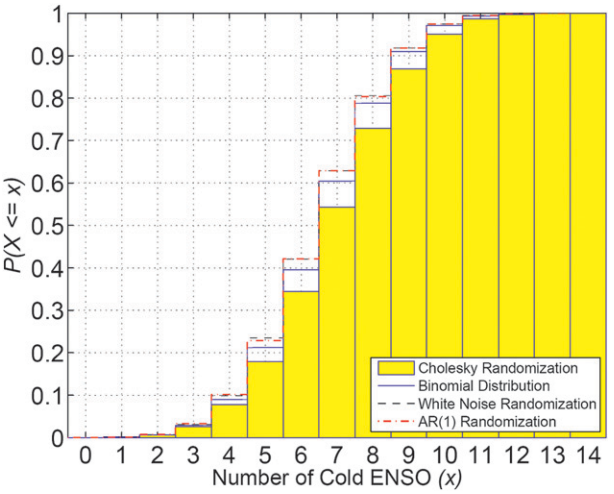

FIG. 5. Cumulative probability distribution of number of cold winters of ENSO-3.4 index at solar peak years from 1860 to 2000. The cumulative distribution was obtained using four methods: 1) randomization using Cholesky's decomposition, so that the expected autocorrelation of the randomized series is the same as the ENSO-3.4 index; 2) binomial distribution; 3) white-noise randomization; and 4) AR(1) randomization. Note that the significance level decreases when the autocorrelation of the ENSO-3.4 index is accounted for. The p value of getting 9 or higher cold stages at 14 SSN peaks, using Cholesky randomization, is $1 - P(X \leq 8) = 1 - 0.73 = 0.27$. The Monte Carlo calculations for white-noise randomization, AR(1) randomization, and Cholesky randomization take into account the presence of the neutral case, and the cold stages are defined as 0.02 unit below its mean (following Roy and Haigh 2012). The analytic formula for the binomial distribution ignores the neutral cases, and the probability of occurrence of either cold or warm ENSO is taken to be 50%.

that carry the same distribution and expected autocorrelation as the observed ENSO time series. The randomized time series are shown in Fig. 3d.

4. Results

The cumulative probability distribution of the randomized time series is shown using the ENSO-3.4 index (Fig. 5) and the cold tongue index (Fig. 6). The ENSO-3.4 index is the same as that used by Roy and Haigh (2012), who chose the December–February average. For the cold tongue index, we use the January–February average; these 2 months were first selected by Van Loon et al. (2007) in their composite. Later, in order to reexamine their work, Zhou and Tung (2010) used the same 2-month average of the cold tongue index to classify ENSO.

Using the ENSO-3.4 index, Roy and Haigh (2012) found that, out of 14 SSN peak years from 1860 to 2000, 9 were cold ENSO, defined as when the index is below 0.02 units of its mean (see Fig. 4). Figure 5 shows that the p value for 9 or higher cold ENSO out of 14 is 0.27 (or at the 73% confidence level). The null hypothesis, thus, cannot be rejected at the 95% confidence level.

Next, we test the robustness of our conclusion to the threshold used to define the cold events by removing the threshold and counting any negative event, no matter how small, as cold. For the ENSO-3.4 index, only one of the neutral events, the first triangle in Fig. 4, is negative (at −0.0154), and thus 10 cold events out of 14 are observed. The p value of getting 10 or higher cold events is 0.14 (figure not shown). For the cold tongue index, there is no neutral case and 8 cold ENSO were observed at 11 solar peak years. The p value of getting 8 or higher cold events is 0.16 from Fig. 6. None of the cold-ENSO occurrences tested carries a p value smaller than 0.05 (i.e., at higher than the 95% significance level), even if we reclassify the neutral years as cold ENSO.

5. Conclusions

We have introduced a statistical method to test the relationship between the peaks of the 11-yr solar cycle and cold equatorial Pacific sea surface temperature (cold ENSO or La Niña). We used surrogate series data that carry the same autocorrelation and distribution as the ENSO series to make sure that the ENSO series and its randomized surrogate possess the same degrees of freedom, frequency content, and expected autocorrelation. Our tests cannot rule out the null hypothesis that cold-ENSO events are not associated with the sunspot numbers at the peak years. The Quinn index, which is a much longer proxy time series than is available in the instrumental record, suggests that cold ENSO and warm ENSO are almost equally distributed

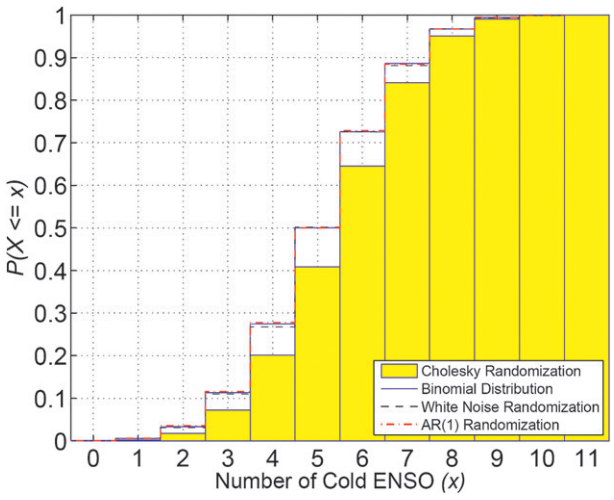

FIG. 6. Cumulative probability distribution of the number of cold winters of the cold tongue index at 11 SSN peak years. The distributions were obtained by randomizing the cold tongue index series using the four methods listed in Fig. 5. The significance level decreases as the autocorrelation of the cold tongue index is accounted for. The p value of getting 8 or higher cold stages, from the Cholesky randomization method, is $1 - P(X \leq 7) = 1 - 0.84 = 0.16$. Cold ENSO is defined as the cold tongue index (or its randomized series) below its mean, with no threshold. For analytical binomial distribution, the probability of being cold ENSO is assumed to be 50%.

at solar peak years and implies that they are an independent phenomena.

Acknowledgments. We thank Jiansong Zhou and Indrani Roy for their helpful discussions. The research is supported by National Science Foundation under Grant DMS 0940342 and the National Aeronautics and Space Administration under Grant NNX11AC75G.

REFERENCES

Awe, O., 1964: Errors in correlation between time series. *J. Atmos. Terr. Phys.,* **26,** 1239–1255.

Devroye, L., 1986: *Non-Uniform Random Variate Generation*. Springer-Verlag, 843 pp.

Haam, E., and P. Huybers, 2010: A test for the presence of covariance between time-uncertain series of data with application to the Dongge Cave speleothem and atmospheric radiocarbon records. *Paleoceanography,* **25,** PA2209, doi:10.1029/2008PA001713.

Lean, J., G. J. Rottman, J. Harder, and G. Kopp, 2005: SORCE contributions to new understanding of global change and solar variability. *Sol. Phys.,* **230,** 27–53.

Meehl, G. A., and J. M. Arblaster, 2009: A lagged warm event–like response to peaks in solar forcing in the Pacific region. *J. Climate,* **22,** 3647–3660.

——, ——, K. Matthes, F. Sassi, and H. Van Loon, 2009: Amplifying the Pacific climate system response to a small 11-year solar cycle forcing. *Science,* **325,** 1114–1118.

Misios, S., and H. Schmidt, 2012: Mechanisms involved in the amplification of the 11-yr solar cycle signal in the tropical Pacific Ocean. *J. Climate,* **25,** 5102–5118.

Ortlieb, L., 2000: The documented historical record of El Niño events in Peru: An update of the Quinn record (sixteen through nineteenth centuries). *El Niño and the Southern Oscillation: Multiscale Variability and Global and Regional Impacts,* H. F. Diaz and V. Markgraf, Eds., Cambridge University Press, 207–295.

Percival, D. B., and A. T. Walden, 1993: *Spectral Analysis for Physical Applications: Multitaper and Conventional Univariate Techniques*. Cambridge University Press, 583 pp.

Quinn, W. H., 1992: A study of Southern Oscillation-related climate activity for A.D. 622–1900 incorporating Nile River flood data. *El Niño: Historical and Paleoclimatic Aspects of the Southern Oscillation,* H. F. Diaz and V. Markgraf, Eds., Cambridge University Press, 119–149.

Rapp, P. E., A. M. Albano, I. D. Zimmerman, and M. A. Jiménez-Montaño, 1994: Phase-randomized surrogates can produce spurious identifications of non-random structure. *Phys. Lett.,* **A192,** 27–33.

Roy, I., and J. D. Haigh, 2010: Solar cycle signals in sea level pressure and sea surface temperature. *Atmos. Chem. Phys.,* **10,** 3147–3153.

——, and ——, 2012: Solar cycle signals in the Pacific and the issue of timings. *J. Atmos. Sci.,* **69,** 1446–1451.

Schreiber, T., and A. Schmitz, 1996: Improved surrogate data for nonlinearity tests. *Phys. Rev. Lett.,* **77,** 635–638.

——, and ——, 2000: Surrogate time series. *Physica D,* **142,** 346–382.

Theiler, J., S. Eubank, A. Longtin, B. Galdrikian, and J. Farmer, 1992: Testing for nonlinearity in time series: The method of surrogate data. *Physica D,* **58,** 77–94.

Tung, K.-K., and J. Zhou, 2010: The Pacific's response to surface heating in 130 years of SST: La Niña–like or El Niño–like? *J. Atmos. Sci.,* **67,** 2649.

Van Loon, H., and G. A. Meehl, 2008: The response in the Pacific to the sun's decadal peaks and contrasts to cold events in the Southern Oscillation. *J. Atmos. Sol. Terr. Phys.,* **70,** 1046–1055.

——, ——, and D. J. Shea, 2007: Coupled air-sea response to solar forcing in the Pacific region during northern winter. *J. Geophys. Res.,* **112,** D02108, doi:10.1029/2006JD007378.

White, W. B., and Z. Liu, 2008: Non-linear alignment of El Niño to the 11-yr solar cycle. *Geophys. Res. Lett.,* **35,** L19607, doi:10.1029/2008GL034831.

Wunsch, C., 1999: The interpretation of short climate records, with comments on the North Atlantic and Southern Oscillations. *Bull. Amer. Meteor. Soc.,* **80,** 245–255.

Zhou, J., and K.-K. Tung, 2010: Solar cycles in 150 years of global sea surface temperature data. *J. Climate,* **23,** 3234–3248.